https://doi.org/10.17221/141/2020-VETMED

Comparative analysis of the exosomal contents of DF-1 cells infected by ALV-J

*Jie Yang, Pingping Zhuang, Ziqiang Cheng, Guihua Wang**

Department of Fundamental Veterinary, College of Veterinary Medicine, Shandong Agricultural University, Tai'an, China

**Corresponding author: wguihua1126@163.com*

Citation: Yang J, Zhuang P, Cheng Z, Wang G (2022): Comparative analysis of the exosomal contents of DF-1 cells infected by ALV-J. Vet Med-Czech 67, 87–98.

Abstract: Exploration of the abnormal expression of exosomal molecules during the infection of avian leukosis virus subgroup J (ALV-J) is essential to provide a deeper understanding of the exosome's role in the viral pathogenesis involved. The study aimed to investigate the differentially expressed proteins and miRNAs of the exosomes derived from DF-1 cells infected by ALV-J, their gene function and involved signal pathways. We isolated exosomes from DF-1 cells infected by ALV-J. The differentially expressed proteins and miRNAs of the exosomes were determined by proteomics and transcription detection technology. A Gene Ontology (GO) analysis and a Kyoto Encyclopedia of Genes and Genomes (KEGG) signal pathway analysis identified the miRNAs target genes and the signal pathways regulated by the different proteins or/and miRNAs. A total of 116 proteins (58 upregulated and 58 downregulated) and 3 miRNAs (all upregulated) were determined. These proteins were involved in 155 signal pathways, in which the highest number of proteins involved in the cancer pathway was (up to) seven. The target genes of the miRNAs were involved in 3 signal pathways. Both the proteins and target genes of the miRNAs were involved in the Ribosome pathway and ECM-receptor interaction pathway. The results suggested that the ALV-J infection changed the proteins and miRNAs of the exosomes significantly.

Keywords: avian leukosis virus subgroup J (ALV-J); exosomes; proteomics; transcriptomics

Avian leukosis virus subgroup J (ALV-J) is an oncogenic retrovirus that mainly induces immunosuppression (Payne et al. 1991). The pathogenesis of ALV-J is still unclear. We found that exosomes from DF-1 cells infected by ALV-J play an important role in pathogenesis because of carrying important viral proteins (Wang et al. 2017). Exosomes, as a membranous nanovesicles, play pivotal roles in both the physiological and disease pathogenesis (Momen-Heravi et al. 2014). Exosomes exert their biological or pathophysiological functions by delivering diverse bio-macromolecules including miRNAs, mRNA, proteins, and lipids (Montecalvo et al. 2012; Marimpietri et al. 2013; Khan et al.

Supported by the National Natural Science Foundation of China (31101789), and Pension Fund for Young and Middle-Aged Scientists of Shandong Provincial (BS2013SW016).

https://doi.org/10.17221/141/2020-VETMED

2016). The different exosomal functions depend on the composition and derived cells of the exosomes (Poveda and Freeman 2017). The exosome's biological functions were significantly determined by the horizontal transfer of their cargoes between cells (Khatri et al. 2018).

The effect of an ALV-J infection on the cargoes of the exosomes and the functions of the exosomes in the pathogenesis of ALV-J are not clear. In this study, we analysed the proteins and miRNA of exosomes and determined the differential exosomal proteins and miRNAs from ALV-J infected DF-1 cells.

Furthermore, the associated biological processes and function enrichment classification of the proteins and miRNA target gene were analysed by integrated target prediction.

MATERIAL AND METHODS

Cells, virus and exosomes

DF-1 cells were cultured in Dulbecco's modified Eagle medium (DMEM), and infected by ALV-J as previously reported (Dong et al. 2015a; Dong et al. 2015b). We used a $TCID_{50}$ (median tissue culture infectious dose) of the ALV-J to infect the cells. The $TCID_{50}$ of the ALV-J (Chinese strain: NX0101) maintained in our laboratory was $10^{3.75}$/ml. The cells' infection was analysed with indirect immunofluorescence assays (IFA) (Wang et al. 2017). Exosomes were isolated using a Total Exosome Isolation Reagent (from the cell culture media) (Invitrogen, Carlsbad, USA) based on the manufacturer's protocol. The exosome samples were previously prepared by our lab (Wang et al. 2017). Three independent samples were conducted for the statistical analysis. The isolated exosomes were identified by electron microscopy observation.

Comparative quantitative proteomic (iTRAQ) analysis of exosomes

A Q Exactive (Thermo Fisher Scientific, Rockford, IL, USA) high-resolution mass spectrometer was used for the exosomal quantitative proteomic analysis and was performed per a previously reported protocol (Wang et al. 2017). The quantitative sequence information of the proteins was extracted from the UniProtKB database (Version No. 201602).

Compared with the control, the proteins with a fold change of expression > 1.2 (up/downregulation) and a *P*-value < 0.05 were determined as differentially expressed proteins.

Transcriptome analysis of the exosomes

The total RNA of the exosomes was isolated from the exosomes using a Total Exosome RNA and Protein Isolation Reagent (Invitrogen, Carlsbad, USA). Illumina small RNA deep sequencing was performed as described in a previous study (Zhou et al. 2018). The genome comparison analysis software Bowtie v1.1.2 (Langmead et al. 2009) was used to identify the known miRNAs according to the genome annotation information in the miRBase database (release 21). For those miRNAs that did not match with known sequences, the software miRDeep2 was used to predict the new miRNAs (Friedlander et al. 2012). The software DESeq was used to analyse the differences in the miRNA expression levels. The screening conditions for the differential miRNA were $P < 0.05$, and $|\log2(\text{Fold\_change})| \geq 1$ (Anders and Huber 2010). The targets of the differentially expressed miRNA were predicted by miRanda v3.3a.

Gene enrichment and functional annotation analysis

Gene enrichment and functional annotation analyses of the screened differential proteins and target genes of the differential miRNAs were conducted through Gene Ontology [(GO); www.geneontology.org)] and Kyoto Encyclopedia of Genes and Genomes [(KEGG), http://www.genome.jp/kegg].

RESULTS

DF-1 cells were infected by ALV-J

The results of the IFA showed that significant green fluorescence was observed around the nucleus of the infected cells compared with the uninfected DF-1 cells (Figure 1).

https://doi.org/10.17221/141/2020-VETMED

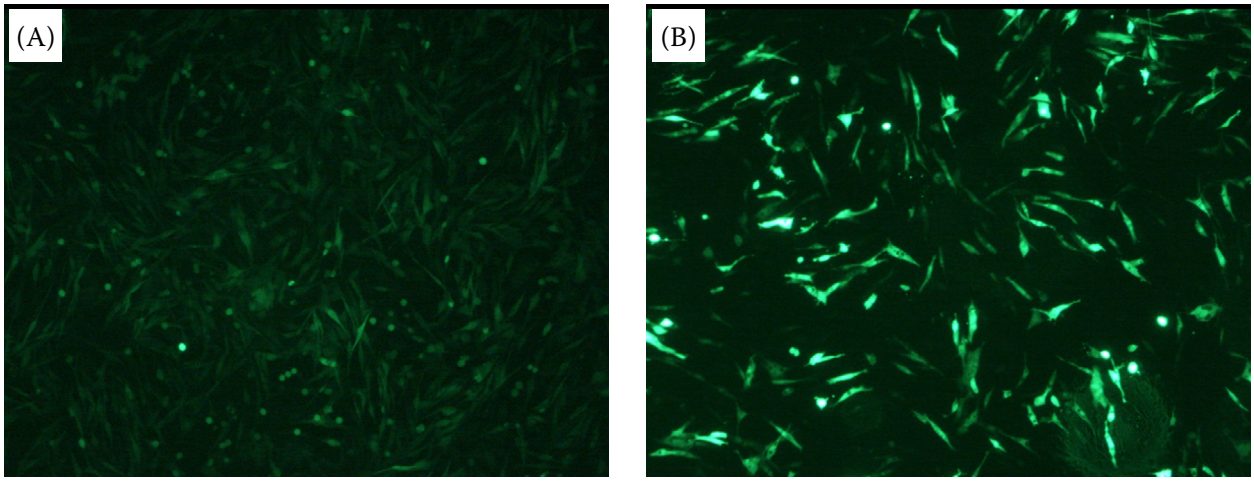

Figure 1. Detection of ALV-J in infected DF-1 cells by IFA
(A) Uninfected DF-1 cells were used as control. (B) Significant green fluorescence was observed in the cytoplasm of the ALV-J infected cells
ALV-J = avian leukosis virus subgroup J; IFA = immunofluorescence assays

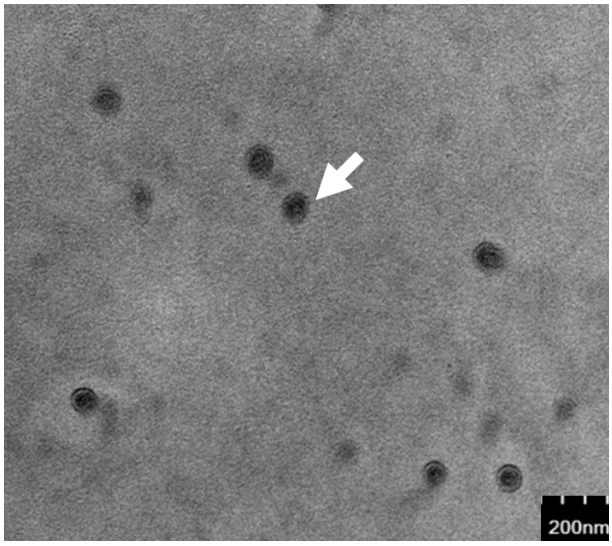

Figure 2. The identification of the prepared exosomes
The size of cup shape vesicles was 100–150 nm under electron microscope observation

Function enrichment analysis of the differential proteins

The isolated exosomes were cup shape vesicles (Figure 2) 100–150 nm in size under electron microscope examination. Through the comparative quantitative proteomic analysis, compared with the exosomes from the uninfected DF-1 cells, 116 proteins in the exosomes from the ALV-J infected cells were screened as differentially expressed proteins ($P < 0.05$), 58 of which were upregulated and 58 were downregulated (Table 1).

Furthermore, a GO function enrichment analysis was carried out for the determined differential proteins. According to the statistics of the proteins at the second level of GO, as shown in Figure 3, these determined proteins were divided into nine categories, including organelles, macromolecular complexes, membrane proteins, extracellular matrices, membrane enclosed lumen proteins, viral proteins, and covered nine molecular activities, and participated in fifteen biological processes, such as metabolic, biological regulation, cellular component organisation or biogenesis, localisation, response to stimulus, developmental, signal, biological adhesion, immune system, growth, and locomotion (Figure 3).

By the KEGG annotation analysis, a total of 155 signal pathways were involved in which these differential proteins participated in. There were 26 pathways in which more than three proteins were involved simultaneously, and the number of proteins involved in the cancer pathway is up to seven (Table 2 and Figure 4).

Target gene prediction and function enrichment analysis of the different miRNA

Through analysis of the differences in the miRNA expression levels, three known miRNAs with $P < 0.05$ and $|\log2(\text{Fold\_change})| \geq 1$ were determined. The expression of miRNA-2954 was 3.90-fold higher, miRNA-365-2-5p was 6.59-fold

https://doi.org/10.17221/141/2020-VETMED

Table 1. Differentially expressed proteins in exosomes from ALV-J (avian leukosis virus subgroup J) infected DF-1 cells

No.	Accession	Protein name	Change	Fold
1	F1NUA2	Actin-related protein 2/3 complex subunit 5 (ARPC5)	up	2.38
2	E1BXS2	Guanine nucleotide-binding protein G subunit alpha-1 (GNAI1)	up	1.65
3	Q64997	Envelope protein subgroup J OS = avian leukosis virus (HPRS103)	up	2.21
4	R4QXY1	Gag and reverse transcriptase polyprotein	up	2.25
5	Q5ZJV5	Cytochrome c oxidase subunit 4I1 (COX4I1)	up	1.57
6	E1C2U6	Protein kinase cAMP-dependent type I regulatory subunit beta (PRKAR1B)	up	1.68
7	Q64996	Gag proteins OS=Avian leukosis virus (HPRS103)	up	1.73
8	E1BR10	Peroxiredoxin 3 (PRDX3)	up	1.47
9	E1BSH9	Betaine-homocysteine S-methyltransferase (BHMT)	up	1.47
10	R4GLK3	LOC100857577	up	1.45
11	Q90922	Netrin-1 (NTN1)	up	1.40
12	H9KZP2	Keratin 8 (KRT8)	up	1.32
13	F1N8F4	Tenascin (TNC)	up	1.42
14	E1BXE8	Transporter (SLC6A11)	up	1.43
15	Q8UWG7	60S ribosomal protein L6 (RPL6)	up	1.33
16	P23991	Alcohol dehydrogenase 1 (ADH1)	up	1.44
17	F1NC27	RAB21, member RAS oncogene family	up	1.33
18	E1BSV7	YKT6	up	1.29
19	E1BVS1	E3 ubiquitin-protein ligase (ITCH)	up	1.30
20	H9L2J4	Drebrin like (DBNL)	up	1.36
21	E1BUD7	LOC100859766	up	1.47
22	R4R035	Envelope polyprotein	up	1.45
23	F1NDN5	Keratin 15 (KRT15)	up	1.34
24	Q02020	Fibrinogen beta chain (FGB)	up	1.35
25	F1NDN6	Keratin 12 (KRT12)	up	1.36
26	E1C4R5	Sodium voltage-gated channel alpha subunit 1 (SCN1A)	up	1.30
27	E1BXR1	VHL binding protein 1 (VBP1)	up	1.33
28	E1C7S2	Hydroxysteroid dehydrogenase like 2 (HSDL2)	up	1.36
29	F1NLH8	DnaJ heat shock protein family (Hsp40) member A4 (DNAJA4)	up	1.31
30	E1C458	CTP synthase (CTPS)	up	1.29
31	F1NA86	Sequestosome 1 (SQSTM1)	up	1.29
32	F1NB64	Acetyl-CoA acyltransferase 1 (ACAA1)	up	1.27
33	F1NNQ3	Vacuolar protein sorting-associated protein 29 (VPS29)	up	1.34
34	E1BZK3	Solute carrier family 12 member 4 (SLC12A4)	up	1.29
35	F1NZC6	Phosphoribosyl pyrophosphate synthase-associated protein 2 (PRPSAP2)	up	1.41
36	F1N9J4	60S ribosomal protein L22 (RPL22)	up	1.35
37	F1NSI3	Cytochrome b5 type B (CYB5B)	up	2.00
38	P13944	Collagen alpha-1(XII) chain (COL12A1)	up	1.45
39	P41125	60S ribosomal protein L13 (RPL13)	up	1.58
40	Q5ZK19	Dynactin subunit 3 (DCTN3)	up	1.30
41	E1BVX9	Signal recognition particle subunit SRP72 (SRP72)	up	1.41
42	Q7ZTS9	Dimethylarginine dimethylaminohydrolase I	up	1.74
43	E1C2I9	Leucyl-tRNA synthetase (LARS)	up	1.29
44	P84172	Elongation factor Tu, mitochondrial (fragment) (TUFM)	up	1.30
45	P19352	Tropomyosin beta chain (TPM2)	up	1.28
46	F1P4F4	Signal sequence receptor subunit 1 (SSR1)	up	1.48
47	F6QGI8	Fructose-bisphosphatase 1 (FBP1)	up	1.28

https://doi.org/10.17221/141/2020-VETMED

Table 1 to be continued

No.	Accession	Protein name	Change	Fold
48	F1P1I4	Serine incorporator 3 (SERINC3)	up	1.46
49	E1C9I8	Transcription factor like 5 (TCFL5)	up	1.44
50	F1NZY9	NADH-cytochrome b5 reductase (CYB5R3)	up	1.31
51	P48440	Dolichyl-diphosphooligosaccharide-protein glycosyltransferase 48 kDa subunit (DDOST)	up	1.47
52	P08629	Thioredoxin (TXN)	up	1.32
53	F1P0A1	X-prolyl aminopeptidase 1 (XPNPEP1)	up	2.33
54	E1BSP8	SEC24 homolog D, COPII coat complex component (SEC24D)	up	2.00
55	E1BZM5	Component of oligomeric golgi complex 7 (COG7)	up	1.38
56	E1BXG9	Peptidylprolyl isomerase D (PPID)	up	1.50
57	F1NW50	ATPase H+ transporting V1 subunit H (ATP6V1H)	up	1.55
58	F1NV89	WD repeat domain 11 (WDR11)	up	1.32
59	F1NYZ7	Chloride intracellular channel 4 (CLIC4)	down	0.79
60	F1P1G6	Cell migration inducing hyaluronidase 1 (KIAA1199)	down	0.72
61	F1P0X1	Mortality factor 4 like 1 (MORF4L1)	down	0.74
62	Q90612	Collagen type III alpha 1 chain (COL3A1)	down	0.80
63	E1BW98	G protein subunit beta 4 (GNB4)	down	0.81
64	R4GGQ4	Translocase of inner mitochondrial membrane 13 (TIMM13)	down	0.73
65	E1C840	Stonin 2 (STON2)	down	0.43
66	F1NHI4	Superoxide dismutase 3 (SOD3)	down	0.80
67	R4GFV3	Microfibril associated protein 5 (MFAP5)	down	0.80
68	F1N8W3	Periostin (POSTN)	down	0.81
69	E1BRE9	Decorin (DCN)	down	0.80
70	F1NP51	Lamin-B2 (LMNB2)	down	0.81
71	Q6EE33	S-(hydroxymethyl)glutathione dehydrogenase (fragment)	down	0.81
72	E1C5F3	Sulfotransferase (CHST6)	down	0.80
73	F1P150	Glypican-1 (GPC1)	down	0.75
74	F1P4N9	Periostin (POSTN)	down	0.79
75	P24367	Peptidyl-prolyl *cis-trans* isomerase B (PPIB)	down	0.78
76	E1C353	Collagen alpha-1(VIII) chain (COL8A1)	down	0.78
77	E1C836	Platelet derived growth factor receptor like (PDGFRL)	down	0.73
78	P43347	Translationally-controlled tumour protein homolog (TPT1)	down	0.79
79	F1ND63	ADAMTS like 3 (ADAMTSL3)	down	0.79
80	R4GFV1	LOC100858243	down	0.75
81	F1P4K9	Collagen type XI alpha 1 chain (COL11A1)	down	0.78
82	F1NF80	Phosphopantothenoylcysteine synthetase (PPCS)	down	0.69
83	F1NM72	GNAS complex locus (GNAS)	down	0.73
84	E1C7E1	Reactive intermediate imine deaminase A homolog (HRSP12, RIDA)	down	0.80
85	P08250	Apolipoprotein A-I (APOA1)	down	0.76
86	P18660	60S acidic ribosomal protein P1 (RPLP1)	down	0.61
87	H9KZN0	Uncharacterized protein (fragment)	down	0.75
88	F1P2R3	Collagen type IV alpha 1 chain (COL4A1)	down	0.76
89	Q90663	Semaphorin-3D (SEMA3D)	down	0.79
90	Q90796	Alpha-1 type XI collagen (fragment)	down	0.73
91	E1C1V3	Plakoglobin (JUP)	down	0.71
92	E1BRL4	Synaptosomal-associated protein (SNAP23)	down	0.79
93	F1N8Z4	RuvB like AAA ATPase 1 (RUVBL1)	down	0.76
94	E1C6M8	EGF containing fibulin extracellular matrix protein 1 (EFEMP1)	down	0.74

https://doi.org/10.17221/141/2020-VETMED

Table 1 to be continued

No.	Accession	Protein name	Change	Fold
95	R4GIY3	Torsin family 2 member A (TOR2A)	down	0.67
96	A3FB57	Receptor protein tyrosine phosphatase LAR (fragment) (RPTPf)	down	0.67
97	Q5F497	RCJMB04_1o11	down	0.74
98	F1NNN7	TNFRSF1A associated via death domain (TRADD)	down	0.75
99	R4GM64	Flavin adenine dinucleotide synthetase 1 (FLAD1)	down	0.80
100	E1BYC6	*N*-acetylglucosamine-1-phosphate transferase subunits alpha and beta (GNPTAB)	down	0.70
101	E1C593	Exportin for tRNA (XPOT)	down	0.71
102	H9L0P9	LOC101751282	down	0.78
103	Q5ZIA3	Sorting nexin 3 (SNX3)	down	0.73
104	Q7T2X3	Low-density lipoprotein receptor (LDLR)	down	0.65
105	F1P2Q3	Collagen type IV alpha 2 chain (COL4A2)	down	0.70
106	E1BTM1	Eukaryotic translation termination factor 1 (ETF1)	down	0.68
107	F1NAM6	Atlastin GTPase 1 (ATL1)	down	0.79
108	Q5ZJ61	Phenylalanyl-tRNA synthetase subunit beta (FARSB)	down	0.69
109	Q5ZM56	Serine/threonine-protein phosphatase 2A activator (PPP2R4)	down	0.67
110	F1NUP9	Short chain dehydrogenase/reductase family 16C member 5 (SDR16C5)	down	0.60
111	F1NP98	Integrin linked kinase (ILK)	down	0.58
112	F1P331	Aldo-keto reductase family 7 member A2 (AKR7A2)	down	0.66
113	F1NK52	Ras homolog family member J (RHOJ)	down	0.51
114	F1P494	Transforming growth factor beta induced (TGFBI)	down	0.53
115	F1P3Q5	Mitogen-activated protein kinase 8 interacting protein 1 (MAPK8IP1)	down	0.36
116	F1NYD7	Exostosin glycosyltransferase 1 (EXT1)	down	0.46

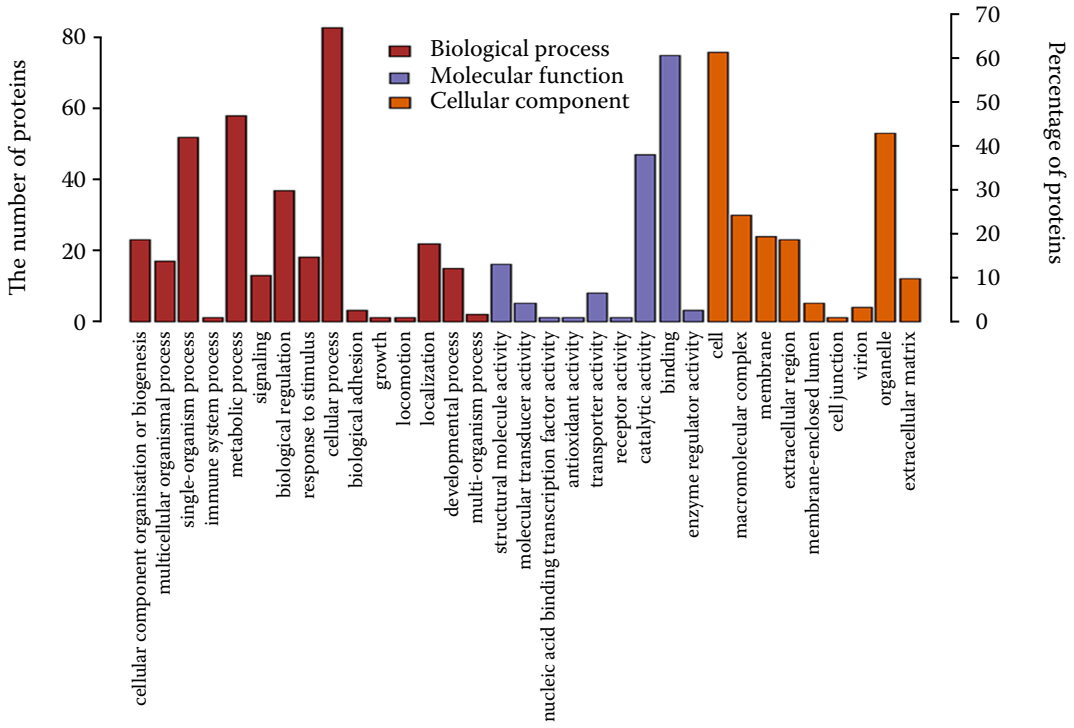

Figure 3. The GO (Gene Ontology) function enrichment analysis of the differentially expressed proteins in the exosomes from the DF-1 cells infected by ALV-J (avian leukosis virus subgroup J)
Exosomes from uninfected cells were used as the control

https://doi.org/10.17221/141/2020-VETMED

Table 2. The number of more than three of the differential proteins involved in the signal pathway and proteins

No.	Map ID	Map name	Protein name and change
1	ko05200	Pathways in cancer	↑: GNAI1, TPM2 ↓: GNB4, GNAS, COL4A1, JUP, COL4A2
2	ko04151	PI3K-Akt signalling pathway	↑: TNC ↓: GNB4, uncharacterised protein (fragment), COL4A1, COL4A2
3	ko04144	Endocytosis	↑: ARPC5, ITCH, VPS29 ↓: SNX3
4	ko00010	Glycolysis/gluconeogenesis	↑: ADH1 ↓: FBP1, S-(hydroxymethyl)glutathione dehydrogenase (fragment)
5	ko03320	PPAR signalling pathway	↑: ACAA1 ↓: uncharacterised protein (fragment), APOA1, ILK
6	ko04728	Dopaminergic synapse	↑: SCN1A, ↓: GNB4, GNAS, RPTPf
7	ko03010	Ribosome	↑: RPL6, RPL22, RPL13 ↓: RPLP1
8	ko04910	Insulin signalling pathway	↑: PRKAR1B ↓: uncharacterised protein (fragment)
9	ko04510	Focal adhesion	↑: no ↓: TNC,COL4A1, COL4A2, ILK
10	ko04611	Platelet activation	↑: E1BXS2, FGB ↓: GNAS, SNAP23
11	ko03013	RNA transport	↑: TUFM ↓: XPOT, LOC101751282
12	ko05034	Alcoholism	↑: E1BXS2 ↓: GNB4, GNAS
13	ko04726	Serotonergic synapse	↑: E1BXS2 ↓: GNB4, GNAS
14	ko04360	Axon guidance	↑: E1BXS2 ↓: NTN1, SEMA3D
15	ko00980	Metabolism of xenobiotics by cytochrome P450	↑: ADH1 ↓: S-(hydroxymethyl)glutathione dehydrogenase (fragment), AKR7A2
16	ko05146	Amoebiasis	↑: no ↓: GNAS, COL4A1, COL4A2
17	ko04974	Protein digestion and absorption	↑: no ↓: COL11A1, COL4A1, COL4A2
18	ko04724	Glutamatergic synapse	↑: E1BXS2 ↓: GNB4, GNAS,
19	ko00071	Fatty acid degradation	↑: ADH1, ACAA1 ↓: S-(hydroxymethyl)glutathione dehydrogenase (fragment)
20	ko00830	Retinol metabolism	↑: ADH1 ↓: S-(hydroxymethyl)glutathione dehydrogenase (fragment), SDR16C5
21	ko04512	ECM-receptor interaction	↑: TNC ↓: COL4A1, COL4A2
22	ko04141	Protein processing in endoplasmic reticulum	↑: SSR1,DDOST, SEC24D ↓: no

https://doi.org/10.17221/141/2020-VETMED

Table 2 to be continued

No.	Map ID	Map name	Protein name and change
23	ko05032	Morphine addiction	↑: E1BXS2 ↓: GNB4 GNAS
24	ko04261	Adrenergic signaling in cardio-myocytes	↑: E1BXS2, P19352 ↓: GNAS
25	ko04931	Insulin resistance	↑: no ↓: uncharacterised protein (fragment), RPTPf, PPP2R4
26	ko04713	Circadian entrainment	↑: E1BXS2 ↓: GNB4, GNAS

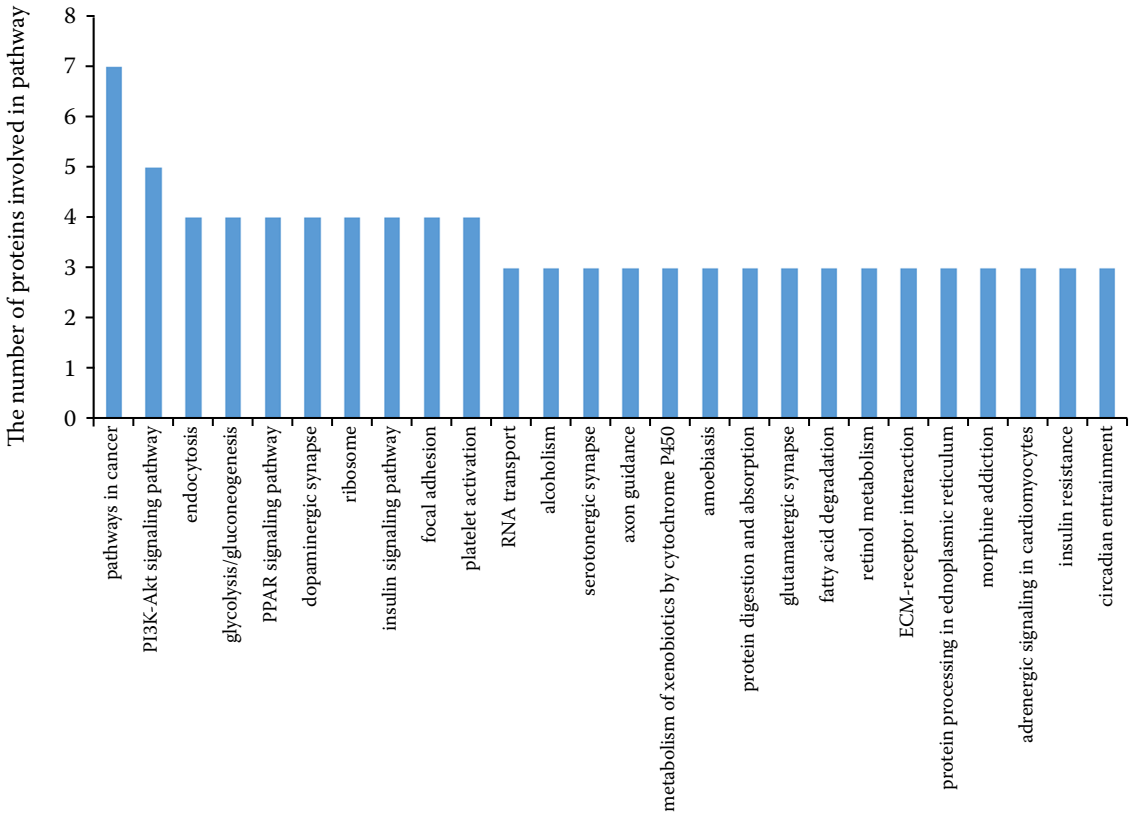

Figure 4. The signal pathways of more than three differentially expressed proteins involved in the process as determined by KEGG (Kyoto Encyclopedia of Genes and Genomes) analysis

higher, and miRNA-146b-5p was 3.29-fold higher (Table 3). No known miRNA with downregulated expression levels were screened.

After the prediction of the three screened differentially expressed miRNA target genes, a GO functional enrichment analysis was performed.

Table 3. The differentially expressed miRNA in the exosome

miRNA	Fold change	*P*-value	FDR	Up/down	Significant
gga-miR-2954	3.90	2.77×10^{-4}	0.042	up	yes
gga-miR-365-2-5p	6.85	3.46×10^{-4}	0.039	up	yes
gga-miR-146b-5p	3.29	3.52×10^{-4}	0.035	up	yes

FDR = false discovery rate

https://doi.org/10.17221/141/2020-VETMED

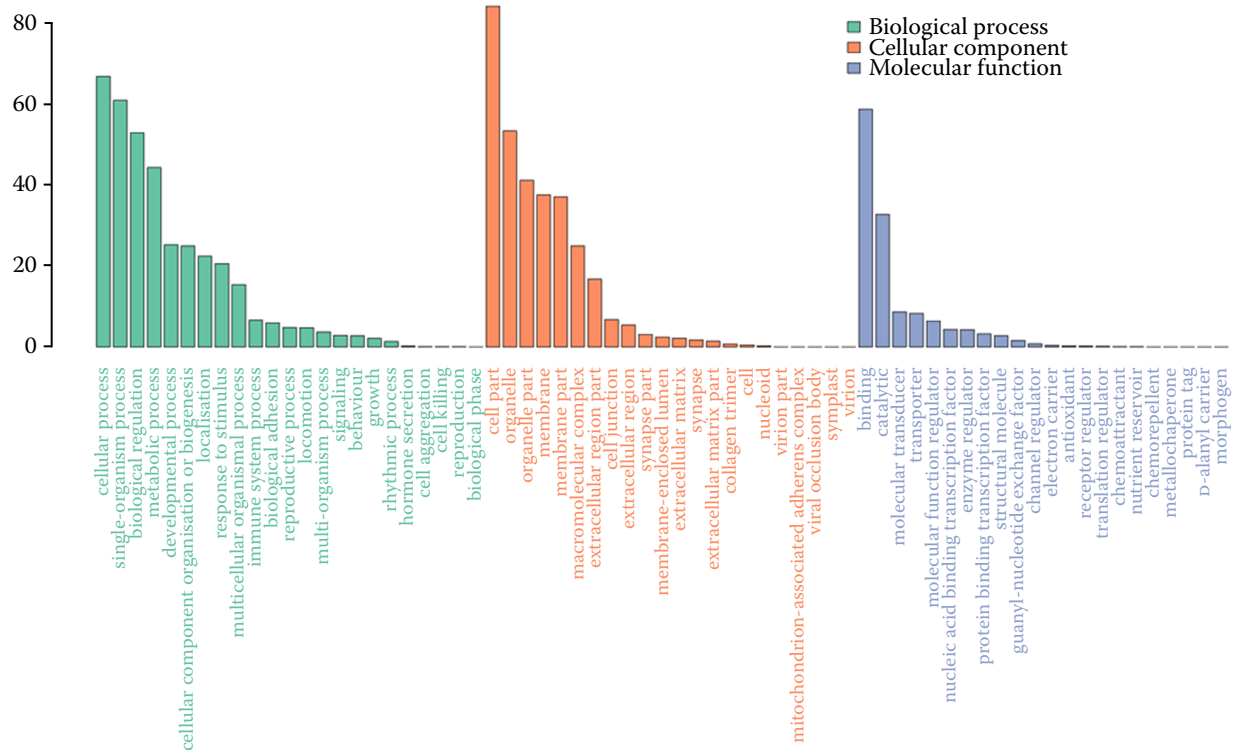

Figure 5. GO (Gene Ontology) term enrichment analysis for the predicted target genes of the different miRNAs in the exosomes

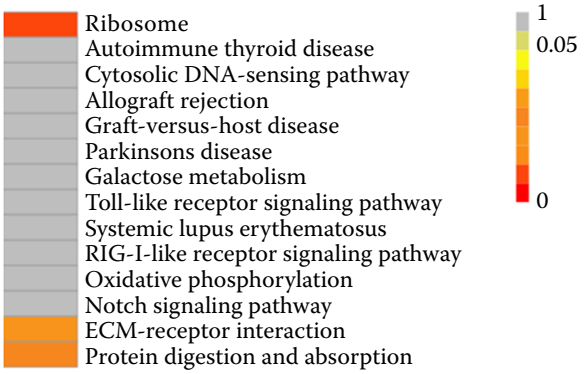

Figure 6. The predicted target genes of the different miRNA in the exosome were analysed by KEGG (Kyoto Encyclopedia of Genes and Genomes)

As shown in Figure 5, the predicted differential target gene components were in 21 categories, including the cell part, organelle, organelle part, membrane, membrane part, macromolecular complex, extracellular region part, cell junction, extracellular region, synapse part, membrane-enclosed lumen, extracellular matrix, synapse, extracellular matrix part, collagen trimer, cell, nucleoid, virion part, mitochondrion-associated adherens complex, viral occlusion body, symplast, and virion. They were involved in the cellular process, single-organism process, biological regulation, metabolic process, developmental process, cellular component organisation or biogenesis, localisation, response to stimulus, multicellular organismal process, immune system process, biological adhesion, reproductive process, locomotion, multi-organism process, signalling, behaviour, growth, rhythmic process, hormone secretion, cell aggregation, cell killing, reproduction, and biological phase.

In order to further analyse the role of the three different miRNAs, putative miRNA target genes were involved in the KEGG pathways using the KEGG PATHWAY Database. We found that the most abundant KEGG terms were included in the ribosome, ECM-receptor interaction, and protein digestion and absorption (Figure 6).

DISCUSSION

This study investigated the differential proteins and miRNA of exosomes from DF-1 cells infected by ALV-J, and the possible mechanism of the exosome's role in the pathogenesis of ALV-J. In an or-

https://doi.org/10.17221/141/2020-VETMED

ganism, proteins do not function independently, but are coordinated by different proteins to perform a series of biochemical or biological function. Therefore, in order to understand the biological process of cells or the mechanism of diseases more systematically and comprehensively, a pathway analysis is usually performed as the most direct and necessary way. In a previous study, we confirmed that exosomes from infected cells possessed immunosuppression due to carrying gag/env proteins of ALV-J (Wang et al. 2017). In this study, the gag/env protein of ALV-J was also detected in the exosome from the DF-1 cells infected by ALV-J (Table 1).

The gag protein was found to promote to the activation of ERK2/AP1 which had a strong correlation with virus associated tumorigenesis. Our results showed that the ALV-J infection affected the signal pathways by changing the composition of the exosomes' proteins, and the pathway in cancer was the most abundant in KEGG terms, which indicated that exosomal proteins play an important role in the neoplasia mechanism of ALV-J. The differentially expressed proteins ARPC5 and Rho-J have been reported to be closely related to the development of various tumours (Kinoshita et al. 2012; Kim et al. 2016). The role and mechanism of the ARPC5 and Rho-J exosomes delivered from cell to cell in ALV-J need to be further studied.

Exosomes contain a wide variety of RNAs such as mRNAs, IncRNAs and miRNAs (Simpson et al. 2012). Among the molecules contained in the exosomes, miRNAs playing regulatory roles in the gene expression have attracted the most attention (Zhang et al. 2015). miRNAs are small non-coding single-stranded RNA molecules that are found to be involved in a variety of physiological and pathological processes, including growth, differentiation, apoptosis, host-pathogen interactions, and cancer (Zhou and Rana 2013; Bhaskaran and Mohan 2014; Hartig et al. 2015; Yu et al. 2017).

In addition, due to the tissue specificity and chronology of miRNA, the expression of miRNA may be different in different tissues or different periods of the same tissues. It has been reported that a reticuloendotheliosis virus and an ALV-J co-infection increased the enrichment of the miRNAs in the exosomes (Zhou et al. 2018). Exosomal miRNAs play an important role in disease progression, since the profiles of the exosomal miRNA may differ from those of the derived cells (Zhang et al. 2015). Therefore, to explore the changes in the miRNAs in exosomes originating from DF-1 cells infected by ALV-J, the function of the changed miRNA target genes and the signal pathway involved will be helpful in revealing the molecular mechanism of ALV-J utilising the exosome pathway causing disease.

miR-2954 and the predicted target genes were reported to affect the thymus immune function of chickens (Zhou et al. 2019), which play an important role in IBV-host interaction and determine the virulence of the infectious bronchitis virus (IBV) strain in kidneys (Yang et al. 2017). miR-365-2-5p was identified in an *in vitro* canine parvovirus infection (Chuammitri et al. 2020). miR-146b-5p and the predicted target genes were associated with breast muscle growth in chickens (Khatri et al. 2018).

To further understand the effects of different miRNAs and the predicted target genes in ALV-J induced immunosuppression and cancer, it is worthwhile to conduct more investigations.

Notably, both the different proteins and target genes of the miRNA were involved in the ribosome pathway and ECM-receptor interaction pathway. The expression of heterogeneous populations of ribosomes in cells and the composition of ribosomes was indicated as being involved in the development of cancer (Bustelo and Dosil 2018; Catez et al. 2019). It has been identified that the ECM-receptor interaction pathway plays an important role in various forms of tumorigenesis (Cao et al. 2018; Li et al. 2018; Bao et al. 2019).

In conclusion, the investigation of exosomal proteins and miRNAs provides novel insights into the function of exosomes in the ALV-J pathogenesis.

Conflict of interest

The authors declare no conflict of interest.

REFERENCES

Anders S, Huber W. Differential expression analysis for sequence count data. Genome Biol. 2010;11(10):R106.

Bao Y, Wang L, Shi L, Yun F, Liu X, Chen Y, Chen C, Ren Y, Jia Y. Transcriptome profiling revealed multiple genes and ECM-receptor interaction pathways that may be associated with breast cancer. Cell Mol Biol Lett. 2019 Jun 6;24(6):38-58.

https://doi.org/10.17221/141/2020-VETMED

Bhaskaran M, Mohan M. MicroRNAs: History, biogenesis, and their evolving role in animal development and disease. Vet Pathol. 2014 Jul;51(4):759-74.

Bustelo XR, Dosil M. Ribosome biogenesis and cancer: Basic and translational challenges. Curr Opin Genet Dev. 2018 Feb;48(2):22-9.

Cao L, Chen Y, Zhang M, Xu DQ, Liu Y, Liu T, Liu SX, Wang P. Identification of hub genes and potential molecular mechanisms in gastric cancer by integrated bioinformatics analysis. PeerJ. 2018 Jul 2;6:e5180.

Catez F, Dalla Venezia N, Marcel V, Zorbas C, Lafontaine DLJ, Diaz JJ. Ribosome biogenesis: An emerging druggable pathway for cancer therapeutics. Biochem Pharmacol. 2019 Jan;159(1):74-81.

Chuammitri P, Vannamahaxay S, Sornpet B, Pringproa K, Patchanee P. Detection and characterization of microRNA expression profiling and its target genes in response to canine parvovirus in Crandell Reese feline kidney cells. PeerJ. 2020 Feb 12;8(2):e8522.

Dong X, Zhao P, Chang S, Ju S, Li Y, Meng F, Sun P, Cui Z. Synergistic pathogenic effects of co-infection of subgroup J avian leukosis virus and reticuloendotheliosis virus in broiler chickens. Avian Pathol. 2015a;44(1):43-9.

Dong X, Zhao P, Li W, Chang S, Li J, Li Y, Ju S, Sun P, Meng F, Liu J, Cui Z. Diagnosis and sequence analysis of avian leukosis virus subgroup J isolated from Chinese Partridge Shank chickens. Poult Sci. 2015b Apr;94(4):668-72.

Friedlander MR, Mackowiak SD, Li N, Chen W, Rajewsky N. miRDeep2 accurately identifies known and hundreds of novel microRNA genes in seven animal clades. Nucleic Acids Res. 2012 Jan;40(1):37-52.

Hartig SM, Hamilton MP, Bader DA, McGuire SE. The miRNA interactome in metabolic homeostasis. Trends Endocrinol Metab. 2015 Dec;26(12):733-45.

Khan MB, Lang MJ, Huang MB, Raymond A, Bond VC, Shiramizu B, Powell MD. Nef exosomes isolated from the plasma of individuals with HIV-associated dementia (HAD) can induce Aβ(1-42) secretion in SH-SY5Y neural cells. J Neurovirol. 2016 Apr;22(2):179-90.

Khatri B, Seo D, Shouse S, Pan JH, Hudson NJ, Kim JK, Bottje W, Kong BC. MicroRNA profiling associated with muscle growth in modern broilers compared to an unselected chicken breed. BMC Genomics. 2018 Sep 17;19(1):683-93.

Kim C, Yang H, Park I, Chon HJ, Kim JH, Kwon WS, Lee WS, Kim TS, Rha SY. Rho GTPase RhoJ is associated with gastric cancer progression and metastasis. J Cancer. 2016 Jul 8;7(11):1550-6.

Kinoshita T, Nohata N, Watanabe-Takano H, Yoshino H, Hidaka H, Fujimura L, Fuse M, Yamasaki T, Enokida H, Nakagawa M, Hanazawa T, Okamoto Y, Seki N. Actin-related protein 2/3 complex subunit 5 (ARPC5) contributes to cell migration and invasion and is directly regulated by tumor-suppressive microRNA-133a in head and neck squamous cell carcinoma. Int J Oncol. 2012 Jun;40(6):1770-8.

Langmead B, Trapnell C, Pop M, Salzberg SL. Ultrafast and memory-efficient alignment of short DNA sequences to the human genome. Genome Biol. 2009;10(3):R25.

Li T, Gao X, Han L, Yu J, Li H. Identification of hub genes with prognostic values in gastric cancer by bioinformatics analysis. World J Surg Oncol. 2018 Jun 19;16(1):114-26.

Marimpietri D, Petretto A, Raffaghello L, Pezzolo A, Gagliani C, Tacchetti C, Mauri P, Melioli G, Pistoia V. Proteome profiling of neuroblastoma-derived exosomes reveal the expression of proteins potentially involved in tumor progression. PLoS One. 2013 Sep 19;8(9):e75054.

Momen-Heravi F, Bala S, Bukong T, Szabo G. Exosome-mediated delivery of functionally active miRNA-155 inhibitor to macrophages. Nanomedicine. 2014 Oct;10(7):1517-27.

Montecalvo A, Larregina AT, Shufesky WJ, Stolz DB, Sullivan ML, Karlsson JM, Baty CJ, Gibson GA, Erdos G, Wang Z, Milosevic J, Tkacheva OA, Divito SJ, Jordan R, Lyons-Weiler J, Watkins SC, Morelli AE. Mechanism of transfer of functional microRNAs between mouse dendritic cells via exosomes. Blood. 2012 Jan 19;119(3):756-66.

Payne LN, Brown SR, Bumstead N, Howes K, Frazier JA, Thouless ME. A novel subgroup of exogenous avian leukosis virus in chickens. J Gen Virol. 1991 Apr;72(Pt 4):801-7.

Poveda E, Freeman ML. Hot news: Exosomes as new players in HIV pathogenesis – New data from the IAS 2017. AIDS Rev. 2017 Oct-Dec;19(3):173-5.

Simpson RJ, Kalra H, Mathivanan S. ExoCarta as a resource for exosomal research. J Extracell Vesicles. 2012 Apr 16;1(4):18374-80.

Wang G, Wang Z, Zhuang P, Zhao X, Cheng Z. Exosomes carring gag/env of ALV-J possess negative effect on immunocytes. Microb Pathog. 2017 Nov;112(11):142-7.

Yang X, Gao W, Liu H, Li J, Chen D, Yuan F, Zhang Z, Wang H. MicroRNA transcriptome analysis in chicken kidneys in response to differing virulent infectious bronchitis virus infections. Arch Virol. 2017 Nov;162(11):3397-405.

Yu Z, Gao X, Liu C, Lv X, Zheng S. Analysis of microRNA expression profile in specific pathogen-free chickens in response to reticuloendotheliosis virus infection. Appl Microbiol Biotechnol. 2017 Apr;101(7):2767-77.

Zhang J, Li S, Li L, Li M, Guo C, Yao J, Mi S. Exosome and exosomal microRNA: Trafficking, sorting, and function.

https://doi.org/10.17221/141/2020-VETMED

Genomics Proteomics Bioinformatics. 2015 Feb;13(1): 17-24.

Zhou D, Xue J, He S, Du X, Zhou J, Li C, Huang L, Nair V, Yao Y, Cheng Z. Reticuloendotheliosis virus and avian leukosis virus subgroup J synergistically increase the accumulation of exosomal miRNAs. Retrovirology. 2018 Jul 3;15(1):45-56.

Zhou Y, Tian W, Zhang M, Ren T, Sun G, Jiang R, Han R, Kang X, Yan F. Transcriptom analysis revealed regulation of dexamethasone induced microRNAs in chicken thymus. J Cell Biochem. 2019 Apr;120(4):6570-9.

Zhou R, Rana TM. RNA-based mechanisms regulating host-virus interactions. Immunol Rev. 2013 May;253(1):97-111.

Received: July 4, 2020
Accepted: September 16, 2021